



Constraining calcification habitat using oxygen isotope measurements in tropical planktonic foraminiferal tests from surface sediments

K.Q. Lakhani^{*}, J. Lynch-Stieglitz, M.M. Monteagudo

School of Earth and Atmospheric Sciences, Georgia Institute of Technology, Atlanta, GA 30332, United States



ARTICLE INFO

Keywords:
Planktonic foraminifera
Apparent Calcification Depth (ACD)
 $\delta^{18}\text{O}$
Tropics

ABSTRACT

Geochemical signals from planktonic foraminiferal tests provide a wide array of tools to investigate past hydrographic changes, but these techniques are limited by our understanding of the habitat at which these organisms form their shell. Quantitative constraints on the variability of the calcification habitat of these organisms can thus lead to better interpretations of these signals and more quantitative constraints on indirect properties related to these signals. We compiled oxygen isotope data from the Tropics to investigate global trends in the apparent calcification depth (ACD) of commonly used planktonic foraminifera. Using *Globigerinoides ruber albus*, *Trilobatus sacculifer*, *Globorotalia tumida*, *Neogloboquadrina dutertrei* and *Pulleniatina obliquiloculata*, we find that our ACD estimates for the global tropics largely match regional ACD estimates from other studies. *G. ruber* and *T. sacculifer* seem to calcify in the surface mixed layer with a mean ACD and 95% confidence interval of 17 [0,86] m and 48 [0,128] m, respectively, and *G. tumida*, *N. dutertrei*, and *P. obliquiloculata* seem to calcify below the mixed layer with a mean ACD of 210 [123,385] m, 114 [42,173] m, and 94 [0,169] m, respectively. The global data set enables the determination of calcification depths across locations with a wide range of thermocline depths. We find that *G. tumida* exhibits a calcification depth that is more spatially invariant, while *N. dutertrei* and *P. obliquiloculata* seem to calcify deeper in the water column in regions where the thermocline is deeper, as has been previously suggested.

1. Introduction

Geochemical signals from foraminiferal tests (fossilized shells) are often used as proxies for environmental variables. Preserved in the sediment record for up to millions of years, these tests can provide insight into how Earth's climate has changed through time. The ratio of oxygen isotopes in the test is primarily correlated with the temperature at which the test formed and the ambient ratio in seawater, allowing for proxy measurements of past ocean temperature given assumptions of the oxygen isotopes in seawater (Emiliani, 1955; Emiliani and Shackleton, 1974; Erez and Luz, 1983). By combining information from shells of multiple species, past water column structure can be inferred (eg. Ford et al., 2018; Mohtadi et al., 2011; Multizzi et al., 1997; Rincón-Martínez et al., 2011; Spero et al., 2003). However, this technique is limited by constraints on foraminiferal habitats. These microorganisms can vertically migrate as they form their tests, resulting in an oxygen isotope record that integrates the conditions of their habitat (Hemleben et al., 1989; Lohmann, 1995). This complex biomimetic process is often simplified as occurring at a single depth, an apparent calcification depth

(ACD) (Hemleben et al., 1989). For a species that can live and record signals over a range of depths, changes in geochemical signals through time can be due to a real climatological change at the presumed depth of calcification, or due to variability in the calcification depth of individual specimens over time. Constraining and understanding ACD variability is critical for extending the use of geochemical signals from subsurface calcifying foraminifera beyond qualitative analyses of vertical ocean structure.

Individual foraminiferal species prefer different ambient conditions, and thus calcify at different depths. Some species, such as *Globigerinoides ruber albus* and *Trilobatus sacculifer*, have obligate photosynthetic symbionts for calcification and other essential functions (Hemleben et al., 1989). These species tend to form most of their calcite test in the photic zone, reflected in their oxygen isotope ratio as more negative. Other species, such as *Neogloboquadrina dutertrei*, choose a habitat based primarily on temperature despite its symbionts (Gastrich, 1987; Ravelo and Andreasen, 1999; Ravelo and Fairbanks, 1992). *N. dutertrei* tends to calcify near the top of the thermocline globally, with regional depth habitat differences that are correlated with thermocline depth (Ravelo

* Corresponding author.

E-mail address: klakhani@gatech.edu (K.Q. Lakhani).

and Andreasen, 1999; Ravelo and Fairbanks, 1992). Foraminifera can also follow reproductive and ecological cues to alter their habitat depth. Reproduction can occur on biweekly, monthly, or yearly cycles depending on the species, and during these cycles, individuals vertically migrate to ensure appropriate conditions for themselves or their offspring (Schiebel and Hemleben, 2017). *G. ruber* spends much of its adult life in the photic zone, but as individuals approach gametogenesis, they migrate deeper towards subsurface chlorophyll maximum layers so that juveniles can acquire dinoflagellate symbionts, as symbionts do not pass from adult to offspring (Brummer et al., 1987; Schiebel and Hemleben, 2017). Many other foraminiferal species engage in similar behavior but calcify differently over this range of depths, resulting in differences in apparent calcification depth. Some species, such as *Globorotalia tumida*, move towards subsurface chlorophyll maximum layers from below for food and reproduction rather than from above (Schiebel and Hemleben, 2005). Some species add a final layer of calcite in the form of a crust, veneer or cortex, sometimes in association with gametogenesis (Lohmann, 1995; Schiebel and Hemleben, 2017; Steinhardt et al., 2015). Ultimately, no species is alike in following the same ecological/environmental cues, yet these are intimately linked to habitat preferences and average depth of calcification.

Understanding the habitat drivers for an individual species allows for an accurate estimate of the calcification habitat for that species and how that habitat could change through time. However, these species can follow multiple drivers, such as temperature, availability of food sources, salinity, pH, reproduction cues, etc. A first step in simplifying this complexity is to distinguish between drivers that are fundamentally linked with depth (such as pressure) and those where the link with depth may change depending on the location (such as the thermocline or chlorophyll maximum layers). There may be some drivers, such as light availability that may be more closely linked with depth in the tropics, although the relationship will change with season, latitude, and turbidity. Other drivers, such as the depth of the nutricline may more directly follow thermocline depth which is highly variable in the tropics, and may have had a different pattern during past climates. In the open ocean, a species that prefers a certain light level will not change its habitat much as climate changes, while a species that prefers to calcify at the same temperature will change its habitat over time in accordance with changes in the isotherm depth. Identifying which of these factors play a larger role in the calcification habitat for a species is a useful first step to identifying and quantifying how these drivers determine the ACD and underlying biomineralization for that species. This knowledge will, in turn, allow for more accurate reconstruction of past ocean conditions based on geochemical measurements on foraminifera.

Here, we compile oxygen isotope data for five tropical planktonic foraminiferal species, *G. ruber albus* (henceforth *G. ruber*), *T. sacculifer*, *G. tumida*, *N. dutertrei*, and *Pulleniatina obliquiloculata*. Calcification depth is inferred based on the modern water column profiles of temperature and the oxygen isotope ratio in seawater, and the paleotemperature equation for calcite. We compute the depth of calcification at each data location and compare with a model in which the calcification follows a specific position within the thermocline. We further investigate the local single-depth model to disentangle these competing influences in setting the calcification depth for *G. tumida*, *N. dutertrei*, and *P. obliquiloculata*.

2. Materials and methods

2.1. Database compilation

We compiled a database of published Holocene and core top tropical planktic foraminiferal shell $\delta^{18}\text{O}$ (Anderson and Mulitza, 2001; Benway et al., 2006; Broecker et al., 2000; Cléroux et al., 2013; Dang et al., 2018; Hollstein et al., 2017; Leech et al., 2013; Leech, 2013; Malevich et al., 2019; Mohtadi et al., 2011; Monteagudo et al., 2021; Ravelo and Fairbanks, 1992; Regenberg et al., 2009; Rincón-Martínez et al., 2011;

Russell et al., 1994; Sagawa et al., 2012; Savin and Douglas, 1973; Schmidt and Mulitza, 2002; Spero et al., 2003; Stainbank et al., 2019; Steph et al., 2009; Waelbroeck et al., 2005; Zhang et al., 2016; Zhang et al., 2019a, 2019b). Also included is previously unpublished *G. tumida* $\delta^{18}\text{O}$ data from four sediment cores in the Central Tropical Pacific. The methods are the same as described for the previously published *G. ruber* data from these sediment cores (Monteagudo et al., 2021).

For this compilation, we include data between 30°S and 30°N. We used as a base for our compilation the MARGO database, and augmented this with both additional data from surface dwelling species and data from the subsurface species that were not compiled by MARGO (Kucera et al., 2005; Waelbroeck et al., 2005). Many methods of age determination were allowed for this compilation, including radiocarbon dating, oxygen isotope stratigraphy, and core top records. Metadata about the age constraints is included in this database using the MARGO database format. For some cores in the Pacific, core tops have been dated to between 4 and 6 ka, and these data are included in the dataset and marked as Chronozone level 6. Duplicate data was removed from this database, as many later papers cite and use data from existing literature, but replicate data for a single location was kept.

The species compiled were *G. ruber*, *T. sacculifer*, *N. dutertrei*, *G. tumida*, and *P. obliquiloculata*. Size fraction information from available sources is included in the metadata. *G. ruber* size fractions range from 250 to 400 μm , *T. sacculifer* size fractions range from 250 to 500 μm , *G. tumida* size fractions range from 315 to 500 μm , *N. dutertrei* size fractions range from 315 to >500 μm , and *P. obliquiloculata* size fractions range from 250 to 500 μm . The database is provided as supplementary information to this article, and also archived at the World Data Center for Paleoclimatology at the National Climatic Data Center.

2.2. Calcification depth calculations

We used a linear paleotemperature equation established using data from (Kim and O'Neil, 1997) for all species: $\delta^{18}\text{O}_c(\text{PDB}) - (\delta^{18}\text{O}_{\text{sw}}(\text{VS-MOW}) - 0.27) = 0.2 * T + 3.25$ (Lynch-Stieglitz et al., 1999). While accurate, species-specific paleotemperature equations have been widely applied and tested for *G. ruber* and *T. sacculifer*, less work has been done to determine the best paleotemperature equation for the other subsurface species (Bemis et al., 1998; Farmer et al., 2007; Mulitza et al., 2003; Spero et al., 2003; Wejnert et al., 2013). The Kim and O'Neil (1997) equation is based on inorganic precipitation and has been applied to each of these species previously, resulting in reasonable apparent calcification depths (Leech et al., 2013; Lynch-Stieglitz et al., 2015; Wejnert et al., 2013). Bemis et al. (1998) cultured the planktonic foraminifera *Orbulina universa* under high and low light conditions. They found the low light equation was very close to the study of Kim and O'Neil (1997), suggesting that this equation may be appropriate for the deeper calcifying foraminifera in this study. They did, however, find that the high light experiments have an offset from the low light experiments of -0.3% and suggest that this equation better fits the data for *G. ruber*. Using a more limited core-top data set from the Atlantic and simultaneously solving for ACD and paleotemperature equation parameters in a Bayesian statistical framework, Farmer et al. (2007) inferred paleotemperature equations for all species considered in this work. They found equations for *G. tumida* and *P. obliquiloculata* that are statistically different from the Kim and O'Neil (1997) equation. For *P. obliquiloculata*, using the Kim and O'Neil (1997) equation as opposed to their species-specific equation results in no significant change in our ACD results, while for *G. tumida*, their species-specific equation yields systematically deeper ACD. Aside from this, our conclusions do not change, and so for consistency, we use the Kim and O'Neil (1997) paleotemperature equation for all species considered.

Along with a paleotemperature equation, temperature and $\delta^{18}\text{O}_{\text{sw}}$ profiles for each location were needed. For these profiles, we use the World Ocean Atlas 2013 (WOA13) annual mean temperature climatology and the $\delta^{18}\text{O}_{\text{seawater}}$ climatology from LeGrande and Schmidt

(2006). While studies using sediment traps or tows where the time of calcification is known have used seasonal climatologies to determine the ACD, we opt for annual climatologies because we cannot constrain the season in which the foraminifera in the core top data set calcified. However, our data is largely from locations where the seasonal differences in flux are small and the seasonal temperature changes are small (Curry et al., 1983; Gibson et al., 2016; Jonkers and Kučera, 2015). Jonkers and Kučera (2015) describe the seasonal fluxes of *G. ruber*, *T. sacculifer*, *N. dutertrei*, and *P. obliquiloculata* using sediment trap data. In places with high mean annual 0–50 m temperatures, these species do not display strong seasonal changes in flux. Using Fig. S6 from Jonkers and Kučera (2015) to estimate temperature ranges for low seasonality for each species, we find that the bulk of our data is from locations with very little change in seasonal flux (85% for *G. ruber*, 82% for *T. sacculifer*, 69% for *N. dutertrei*, and 74% for *P. obliquiloculata*). For these core locations, the maximum deviation from annual mean conditions is also generally small. For the surface ocean (0–50 m), this deviation is less than 2.5 °C for 91% of locations in the Pacific Ocean, less than 2.5 °C for 89% of locations in the Indian Ocean, and less than 3 °C for 86% of locations in the Atlantic Ocean. For the subsurface seasonal temperature changes, we looked at seasonal movement of the 20 °C isotherm. The error we would expect from using the annual mean climatology as opposed to the appropriate seasonal climatology should be bounded by the seasonal change in this isotherm, which is a common proxy for thermocline depth. We find that 90% of our locations have a maximum seasonal isotherm depth deviation of 25 m, 40 m, and 40 m for the Pacific, Indian, and Atlantic oceans relative to annual mean conditions. The uncertainty seen in Fig. 2 and Table 1 are much larger than this, suggesting that this is not a significant source of error. For these reasons, we use the annual mean temperature climatology.

Using the annual climatologies and the paleotemperature equation from above, a field of predicted $\delta^{18}\text{O}_c$ was created. Measured $\delta^{18}\text{O}_c$ data from our compilation was binned into 0.01° by 0.01° grid boxes. This has the effect of matching cores whose location information is stored to different levels of precision by different sources and averaging replicates at the same core site. For the ACD estimate, a vertical profile of predicted $\delta^{18}\text{O}_c$ at the location nearest to each surface sediment measurement in the database was extracted from the full field and compared to the measured $\delta^{18}\text{O}_c$ at this location. The ACD at each data location is the linearly interpolated depth where predicted $\delta^{18}\text{O}_c$ equals observed $\delta^{18}\text{O}_c$. This results in a distribution of depths for each species, shown in Fig. 2. At some locations, the observed $\delta^{18}\text{O}_c$ value is lower than the predicted $\delta^{18}\text{O}_c$ at the surface; the ACD at these locations is set to 0 m.

In this analysis, we choose to focus on apparent calcification depth (ACD) as opposed to the true calcification depth or the true living depth. The depths at which these organisms live and calcify during the totality of their life cycle is determined by the biology and ecology of the individual foraminifer and are of great interest to the community, but the data we compile and report is not very useful for these questions. Due to the complexity of calcification and deposition of shells, the isotope-derived depth may not always reflect these biologically relevant quantities. We know that foraminifera vertically migrate through their lifetime, creating calcite chambers at various stages of their life (Schiebel and Hemleben, 2017). To best represent this, a complex model of partial

calcification at multiple depths would be required, along with the appropriate data to constrain this model. We are not able to do this, as the data compiled is for bulk $\delta^{18}\text{O}_c$. Similarly, some of the species investigated form secondary calcite at a deeper depth and with a different $\delta^{18}\text{O}_c$ than the rest of their calcite (Lohmann, 1995; Steinhardt et al., 2015). As we only compile bulk $\delta^{18}\text{O}_c$ data, we cannot constrain this aspect of calcification. While a single ACD at each location is perhaps not the most relevant quantity for fully understanding the ecology of these organisms which calcify at a variety of times and depths throughout their life cycle, it nonetheless can be of great practical utility when using chemical or isotopic measurements on foraminiferal tests accumulating on the seafloor to reconstruct past environmental conditions.

2.3. Calcification habitat relative to the thermocline

We also quantitatively investigate how the calcification depth for these species is related to the mean annual thermocline depth. To do this, we created a metric, *TP* (Thermocline Position), to reflect position relative to the thermocline using mean annual temperature data from WOA13. Using the temperature at the surface and the temperature at 1000 m, this metric recasts depth in terms of position within the thermocline where *TP* = 0 represents the water column properties below the thermocline at a depth of 1000 m, and *TP* = 1 represents conditions above the thermocline, at the surface. Other *TP* values represent conditions at depth *z* where the temperature equals this fraction of the temperature difference between the surface and 1000 m. For example, if the surface and 1000 m temperature are 25 °C and 5 °C, respectively, the depth at which temperature is 20 °C corresponds to *TP* = 0.8.

$$T(z) = T_{1000} + TP^*(T_0 - T_{1000})$$

For each grid point, there is a 1:1 mapping for depths (0 m–1000 m) to *TP* (0–1), and for a constant *TP* across the tropics, the corresponding depth field has a structure similar to the thermocline depth (Fig. 5d), with the depth at *TP* = 0.8 best approximating the depth of the 20 °C isotherm, a widely used proxy for thermocline depth (Kessler, 1990; Meyers, 1979; Sil and Chakraborty, 2012). The value of *TP* = 0.8 was determined by linearly interpolating the mean annual temperature climatology to determine the depth of the 20 °C isotherm for each location in the tropics and minimizing the RMS error between the depth of the 20 °C isotherm and the depth for each *TP* between 0.50 and 1.00 in increments of 0.01. For locations that are too shallow (bottom depth < 1000 m), the temperature at 1000 m for the nearest grid point was taken. At these locations, *TP* ranges from the *TP* corresponding to the bottom water temperature to *TP* = 1 at the surface.

Using our *TP* metric, we can investigate foraminiferal habitat in this variable space. If a foraminifer calcifies near the top of the thermocline, the best fitting *TP* for that species should be high, and if it calcifies near the bottom of the thermocline, the best fitting *TP* should be low. Similar to our analyses in depth space, at each data location, we identify the *TP* for each species where the measured $\delta^{18}\text{O}_c$ matches the predicted $\delta^{18}\text{O}_c$, iterating *TP* between 0 and 1 in increments of 0.01.

3. Results

This compilation has 991 data points at 728 locations for *G. ruber*, 770 data points at 618 locations for *T. sacculifer*, 273 data points at 209 locations for *G. tumida*, 389 data points at 295 locations for *N. dutertrei*, and 204 data points at 187 locations for *P. obliquiloculata*. These locations span the entire tropics, with most of the data clustering in the Eastern Pacific, the Western Pacific, the coastal Indian Ocean, and the Atlantic Ocean. The full dataset includes verified Late Holocene (0–4 ka), but also data from the mid-Holocene as well as unverified core top data for some locations. This was done to balance the need for enough data for robust conclusions (i.e. there is no verified Holocene data for *P. obliquiloculata* in the Eastern Pacific) and only using data from time

Table 1
Species-specific statistics for Holocene dated data. Confidence Interval is CI.

Species	Local ACD μ (m)	Local ACD 95% (m)	Local Thermocline Position μ	Local Thermocline Position 95% CI
<i>G. ruber albus</i>	17	[0, 86]	0.98	[1.00, 0.86]
<i>T. sacculifer</i>	48	[0, 128]	0.94	[1.00, 0.77]
<i>G. tumida</i>	210	[123, 385]	0.51	[0.80, 0.27]
<i>N. dutertrei</i>	114	[42, 173]	0.73	[0.98, 0.40]
<i>P. obliquiloculata</i>	94	[0, 169]	0.82	[1.00, 0.59]

periods that match modern climatologies. 18.38% of the *G. ruber* data and 0.66% of the *T. sacculifer* data are from the MARGO Late Holocene $\delta^{18}\text{O}$ database (Waelbroeck et al., 2005), and 39.55% of the *G. ruber* data and 58.86% of the *T. sacculifer* data are from Schmidt and Mulitza (2002).

For each species, the $\delta^{18}\text{O}_\text{c}$ for Late Holocene aged samples verified

with age control (0–4 ka, MARGO Chronozones 1–4), hereafter referred to as the Late Holocene data, spans a large range of values, where the range for *G. ruber* is 4.80‰, *T. sacculifer* is 3.76‰, *G. tumida* is 2.96‰, *N. dutertrei* is 4.15‰, and *P. obliquiloculata* is 4.01‰. This variability suggests that each species records changing ocean conditions rather than recording a single isotherm or isopycnal. Late Holocene $\delta^{18}\text{O}_\text{c}$

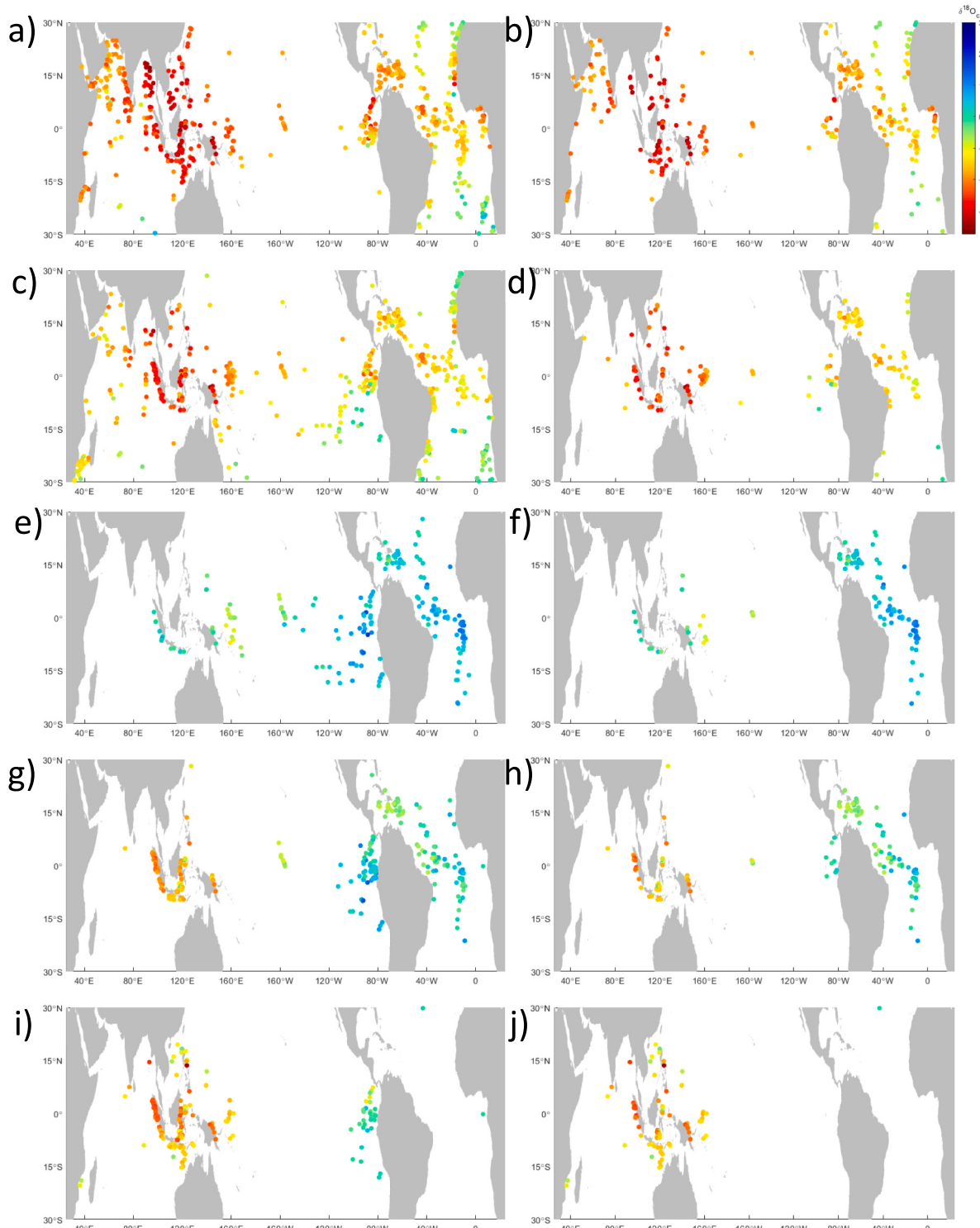


Fig. 1. $\delta^{18}\text{O}_\text{c}$ from compiled dataset. a) Core top dataset for *G. ruber albus* b) Late Holocene dated *G. ruber albus* data, c) Core top dataset for *T. sacculifer*, d) Late Holocene dated *T. sacculifer* data, e) Core top dataset for *G. tumida*, f) Late Holocene dated *G. tumida* data, g) Core top dataset for *N. dutertrei*, h) Late Holocene dated *N. dutertrei* data, i) Core top dataset for *P. obliquiloculata*, j) Late Holocene dated *P. obliquiloculata* data. Color bar signifies range of $\delta^{18}\text{O}_\text{c}$ on a common scale for all species in (‰).

variability, shown in Fig. 1, matches known temperature features, with mixed layer species (*G. ruber* and *T. sacculifer*) having lower $\delta^{18}\text{O}_c$ near the equator and in the western Pacific (corresponding to warmer temperatures) and higher $\delta^{18}\text{O}_c$ in the eastern Pacific and towards the extratropics (corresponding to cooler temperatures). Mixed layer in this context refers to the relatively homogenous layer above the thermocline.

However, also apparent in Fig. 1 is variability in the core top values within regions where the ocean conditions that should drive these values are similar. Some of this variability may be due to the effect of bioturbation, mixing shells from older time periods with more recent shells. This impacts all sediments to some extent but is most important in low sedimentation regions (Boyle, 1984). Independent of habitat changes over time, ice volume changes systematically make glacial aged shells isotopically heavier than modern aged shells.

3.1. Apparent calcification depth

For all species considered in this study, the mean of the local ACD distributions generally matches the results from regional studies (Fig. 2). For *G. ruber* and *T. sacculifer*, the range of local ACD is from 0 to 150 m, but within this range, the distributions suggest that *G. ruber* calcifies closer to the surface than *T. sacculifer*, which other studies have shown (Lynch-Stieglitz et al., 2015; Rincón-Martínez et al., 2011; Steph et al., 2009). 59% of the *G. ruber* data is estimated to be above the surface (and set to 0 m), compared to 22% of *T. sacculifer* data. *N. dutertrei* and *P. obliquiloculata* local ACDs range from 50 to 175 m, with few below these depths. *G. tumida* appears to be the deepest calcifying species, with most local ACD estimates between 125 and 200 m, but with some below 300 m. Only one location for *P. obliquiloculata* has a $\delta^{18}\text{O}_c$ lower than the surface predicted $\delta^{18}\text{O}_c$, while *G. tumida* and *N. dutertrei* have no data above the surface. The subsurface-dwelling species have much more variability in local ACD compared to the surface-dwelling species. These results can be seen spatially in Fig. 3.

3.2. Relationship of calcification to the thermocline

Our local TP estimates are similar to our local ACD estimates, with species calcifying in the same order in the water column (Fig. 4). *G. ruber*

and *T. sacculifer* seem to calcify at $TP \approx 1$, and *P. obliquiloculata*, *N. dutertrei*, and *G. tumida* calcify deeper at lower TP, in that order in the water column. This ordering is consistent with other regional studies (Ford et al., 2018; Mohtadi et al., 2011). The mean TP estimates for each species are shown in Table 1, with the subsurface-dwelling species having much more variability in the local TP distribution. For *P. obliquiloculata*, the data in the shallowest TP bin reflects the fact that, in some locations, this species appears to calcify in the surface mixed layer. The TP value changes slowly with depth near the surface mixed layer, and so data that have a local ACD in the mixed layer would have a TP close to 1.00.

4. Discussion

4.1. Surface-dwelling species

The bulk of the local ACD distribution for *G. ruber* is within the upper 50 m across the tropics, confirming previous studies. *G. ruber* is a cosmopolitan species in the tropical surface ocean with obligate symbionts, making it reliant on sunlight (Hemleben et al., 1989). While 59% of the *G. ruber* values were lighter than the predicted $\delta^{18}\text{O}_c$ at the surface, this is likely due in large part to our use of the paleotemperature equation based on Kim and O'Neil (1997), while there is evidence that the true paleotemperature equation for *G. ruber* may be offset by -0.3% (Bemis et al., 1998). Previous work on *G. ruber* has established its habitat within the surface mixed layer, with many paleoceanographic studies using *G. ruber* $\delta^{18}\text{O}$ as a proxy for sea surface temperatures (e.g. Kucera et al., 2005; Spero et al., 2003). Plankton net tows, sediment trap studies, and core top analyses all find an ACD within the surface mixed layer in specific regions and globally (Curry et al., 1983; Waelbroeck et al., 2005; Watkins et al., 1998).

The mean local ACD for *T. sacculifer* is within the mixed layer at 48 m, with much of the distribution of ACD within the upper 100 m. These results broadly match the results of previous regional ACD estimates (Lynch-Stieglitz et al., 2015; Mohtadi et al., 2011; Rincón-Martínez et al., 2011). Similar to *G. ruber*, *T. sacculifer* bears obligate symbionts and so must live near the surface, and culture experiments show that it can survive over a range of salinity and temperature conditions (Bijma

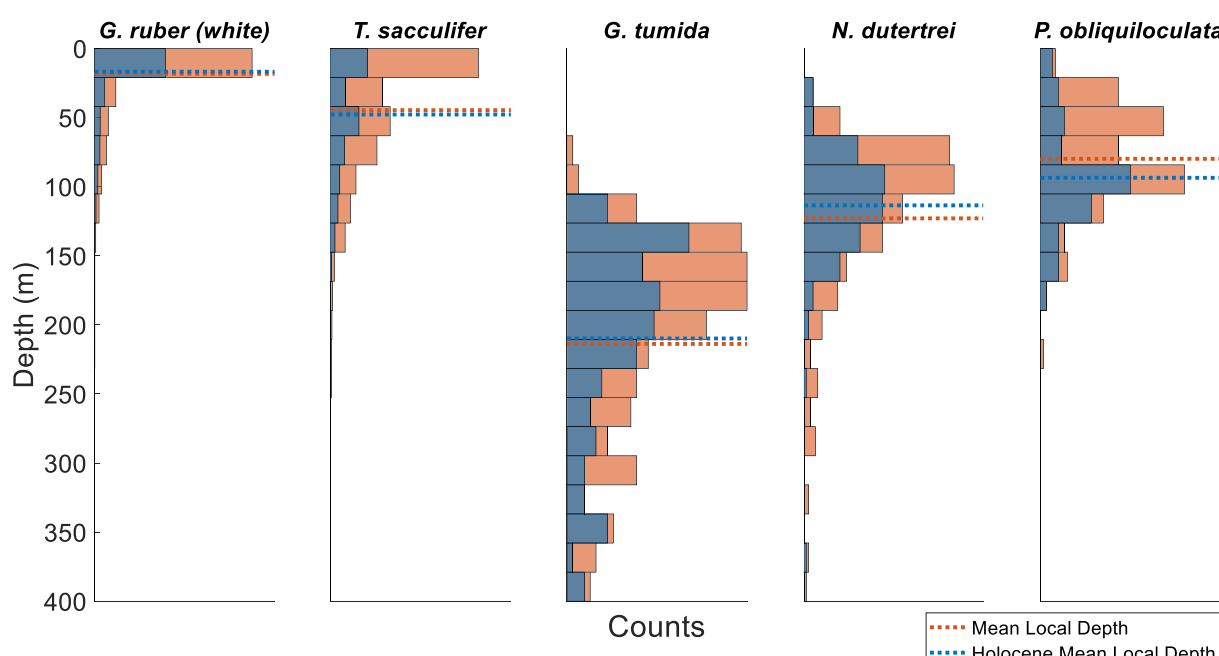


Fig. 2. Local ACD distribution for five tropical planktonic foraminiferal species for the full core top data set and for Late Holocene dated (Chronozone 1–4) data. Dotted line represents mean of local ACD estimates.

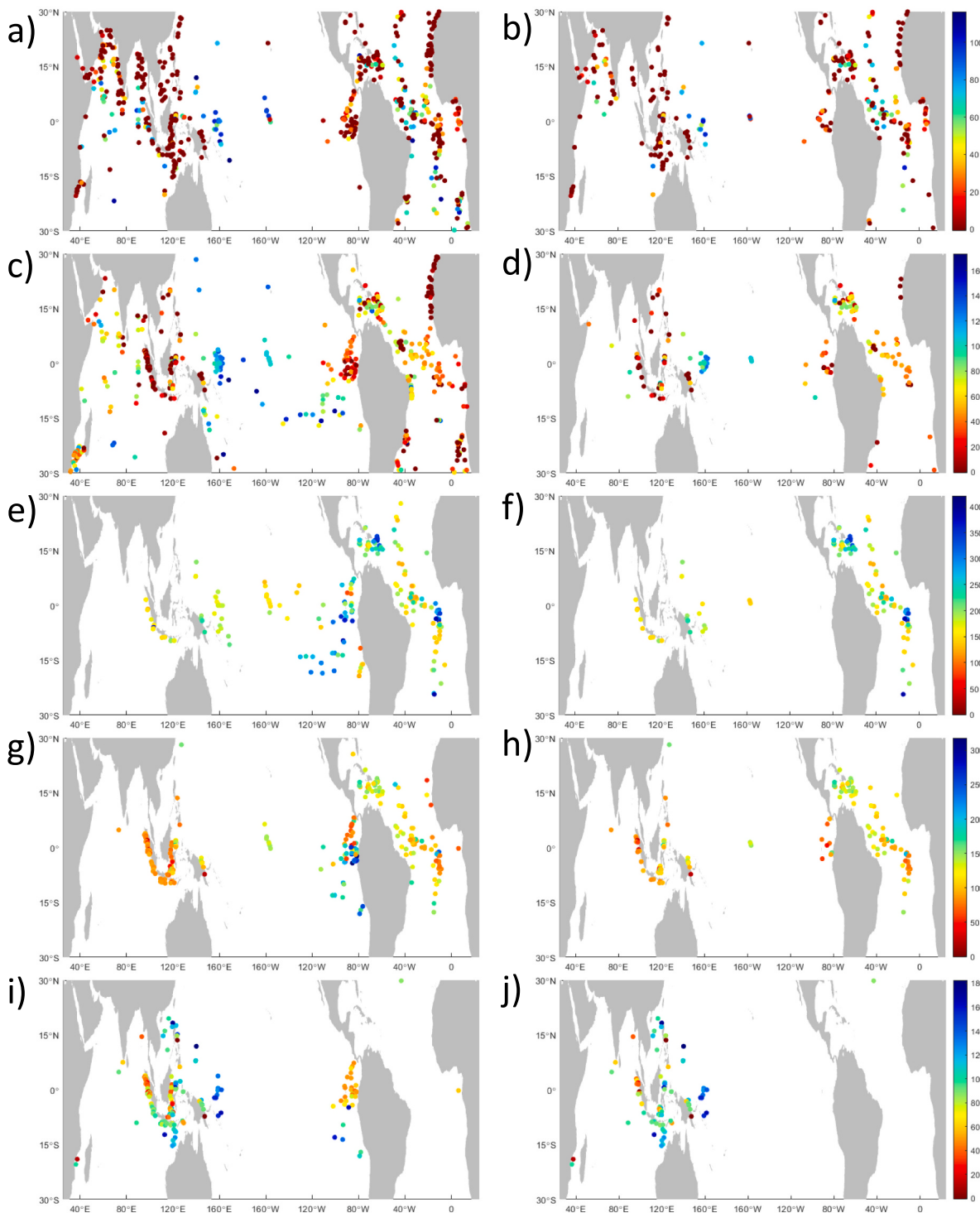


Fig. 3. Local ACD calculated for each species plotted spatially. a) Local ACD from core top dataset for *G. ruber albus* b) Local ACD for Late Holocene dated *G. ruber albus* data, c) Local ACD from core top dataset for *T. sacculifer*, d) Local ACD for Late Holocene dated *T. sacculifer* data, e) Local ACD from core top dataset for *G. tumida*, f) Local ACD for Late Holocene dated *G. tumida* data, g) Local ACD from core top dataset for *N. dutertrei*, h) Local ACD for Late Holocene dated *N. dutertrei* data, i) Local ACD from core top dataset for *P. obliquiloculata*, j) Local ACD for Late Holocene dated *P. obliquiloculata* data. Color bars signify range of local depths for each species in meters.

et al., 1990; Schiebel and Hemleben, 2017). While in regions of steep hydrographic profiles, *T. sacculifer* becomes less reliable as a proxy for surface conditions (Spero et al., 2003), it does record surface conditions well when considered globally.

4.2. Subsurface-dwelling species

The three subsurface species in this study, *G. tumida*, *N. dutertrei*, and *P. obliquiloculata*, live in a more variable environment than the surface-dwelling species. The changing conditions of the thermocline can result in planktonic foraminifera altering their depth habitat for more suitable

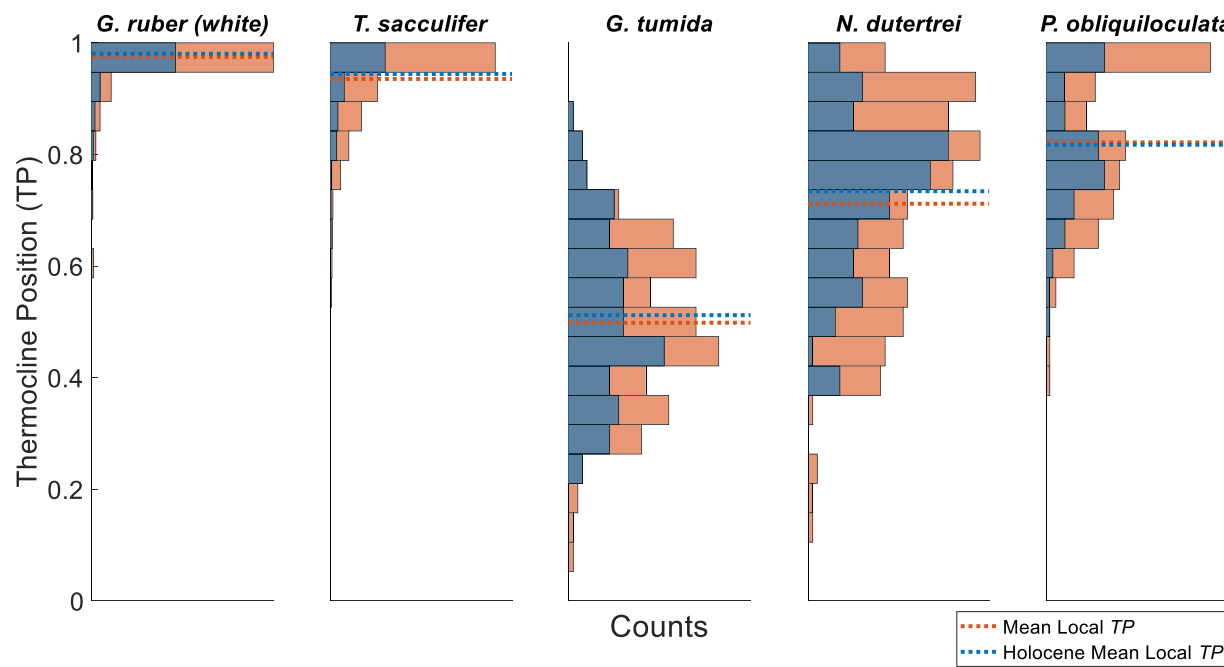


Fig. 4. Local TP distribution for five tropical planktonic foraminiferal species for the full dataset and for Late Holocene dated data. TP = 1 corresponds to the surface, and TP = 0 to 1000 m. Numbers of data points for the full (“core top”) and Late Holocene (“Holocene”) datasets for each species are indicated. Dotted line represents mean of local TP estimates.

conditions, which can lead to systematic errors when these species are used as proxies for past climate. Because many variables tend to change rapidly near the depth of the thermocline, including not only temperature but also density and chlorophyll concentration, it is difficult to disentangle these effects and claim that one is the dominant predictor of habitat depth. Likewise, it is difficult to disentangle which of the many hydrographic properties could drive calcification depth for a species that calcifies independently of the thermocline. Instead, we attempt to identify whether these species calcify independently of the thermocline or calcify at a consistent position in the thermocline.

Fig. 5 shows a comparison between the constant thermocline position (i.e. a foraminifera on average chooses its calcification habitat based on a parameter that tracks the thermocline) and constant depth (i.e. a foraminifera on average calcifies at a fixed depth, independent of thermocline depth) models in explaining $\delta^{18}\text{O}_\text{c}$ variability in *G. tumida*, *N. dutertrei*, and *P. obliquiloculata*. Local ACD is plotted against thermocline depth (depth at which TP = 0.80) to investigate whether the distribution of local ACD changes as a function of thermocline depth. Overlayed on these plots are lines estimating the local ACD assuming either a constant thermocline position or constant depth model. The constant depth is the mean of the local ACD, and the constant TP is the mean of the local TP for the species. For the constant TP line, for each location, the depth for the species' mean TP was estimated, and the line of best fit is plotted. If the foraminifera are primarily responding to a variable that does not change with thermocline depth, the local ACD should be independent of thermocline depth (red line). If the foraminifera are primarily responding to a variable that is linked to the thermocline depth, the local ACD should change as a function of thermocline depth (blue line).

For *G. tumida*, the best fit line for the data matches the constant ACD line most closely, suggesting that calcification depth, while exhibiting a wide range, is independent of thermocline depth. Early work using data from core top sediments to understand the depth habitat of *G. tumida* found that this species calcifies at the Bottom of the Photic Zone (BOPZ) (Ravelo and Andreasen, 1999; Ravelo and Fairbanks, 1992). This BOPZ depth is approximately constant across the tropics (~75–110 m), and is defined as the depth at which light intensity drops to 1% of the surface

intensity (Ravelo and Andreasen, 1999). Since then, some core top studies have confirmed this finding (Steph et al., 2009), while others have estimated the calcification depth to be below the photic zone (Lynch-Stieglitz et al., 2015; Rincón-Martínez et al., 2011). Our results show that *G. tumida* calcifies independently of the thermocline, as Ravelo and Fairbanks (1992) find, but the mean local ACD estimate (210 m) is deeper than the BOPZ, with large variability in the local ACD. This discrepancy in ACD is primarily due to the use of different paleotemperature equations to interpret the data. When our method is used on the data from Ravelo and Fairbanks (1992), we find that the *G. tumida* ACD is deeper than the BOPZ at 230 m at core V29-144. This highlights how different paleotemperature assumptions can lead to differing conclusions for the ACD and thus interpretations of this quantity as a true living or calcification depth.

P. obliquiloculata seem to calcify deeper in regions with deeper thermoclines as opposed to maintaining the same average depth globally (Fig. 5c). This is corroborated by other studies showing that *P. obliquiloculata* calcification is driven by changes in thermocline position (Dang et al., 2018; Zhang et al., 2019b). *P. obliquiloculata* is an herbivorous species, giving it an ecological reason to live and calcify near the deep chlorophyll maximum/deep biomass maximum (Corne et al., 2021; Schiebel and Hemleben, 2017). The highest standing stocks of this species are linked to the pycnocline/thermocline, which is correlated with the deep chlorophyll maximum (Ravelo et al., 1990). Consequently, this species is strongly biased to the upwelling season in the Indo-Pacific and Western Equatorial Pacific (Dang et al., 2018; Kawahata et al., 2002; Mohtadi et al., 2009). Variability in the calcification depth for *P. obliquiloculata* in this study and in other studies is smaller than the variability for other subsurface species (Hollstein et al., 2017; Rippert et al., 2016). This could be due partly because our compilation only has data for this species from the Eastern Equatorial Pacific and the Western Pacific Warm Pool regions, whereas other species have data from a wider variety of environments.

N. dutertrei seems to not calcify at the same average depth independent of thermocline depth, but the change in ACD with thermocline depth does not match our constant thermocline position model either. *N. dutertrei* has been shown to calcify near the bottom of the photic zone

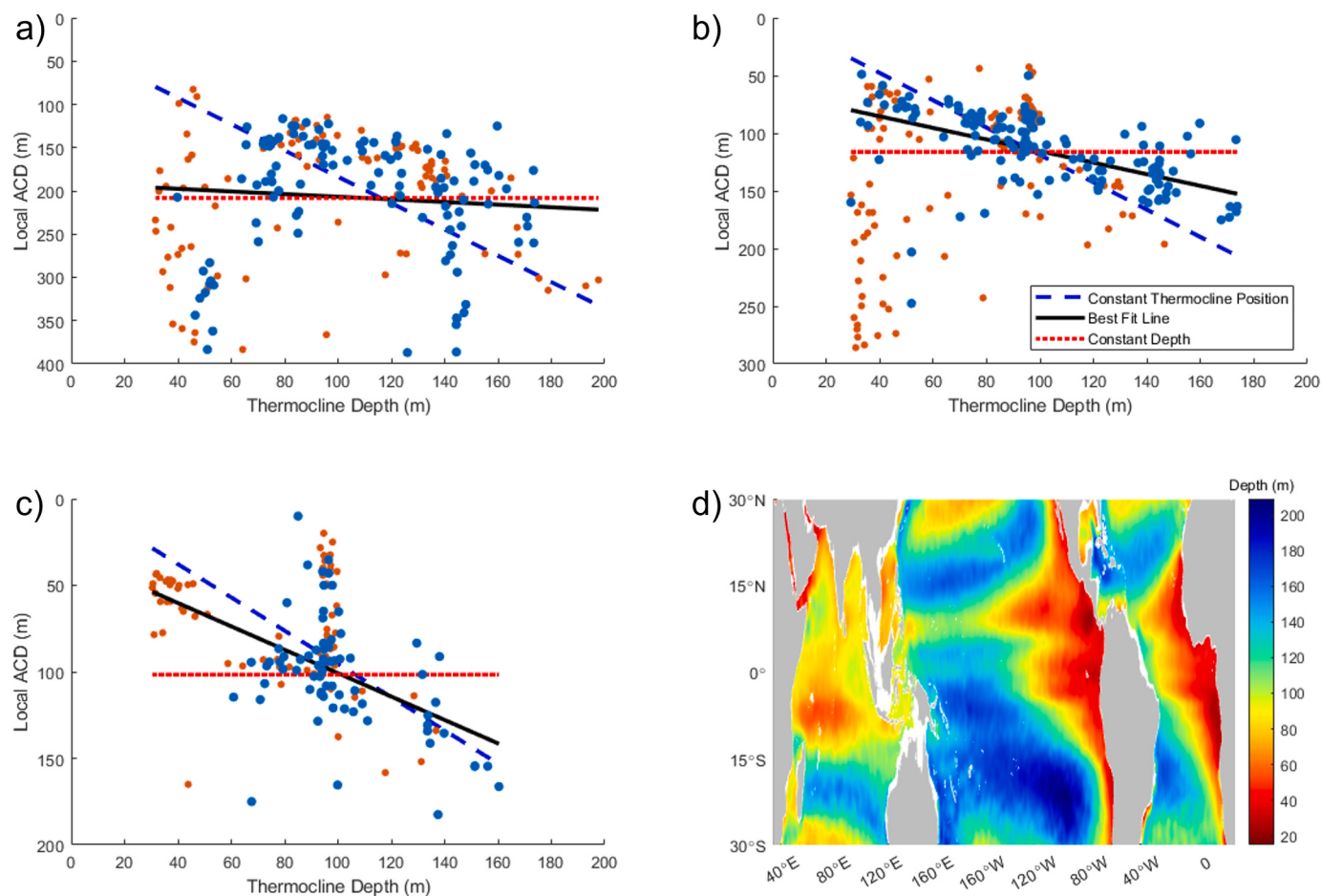


Fig. 5. Local ACD calculated for *G. tumida* (a), *N. dutertrei* (b), and *P. obliquiloculata* (c) as a function of thermocline depth. Late Holocene data is shown in blue, and the full data set including core tops is shown in orange. Lines are best fit local ACD vs. thermocline depth (black), the expected local ACD for a constant average depth calcification (red), and the expected local ACD for a constant average thermocline position (TP) calcification (blue). d) Thermocline depth is defined as the depth where TP = 0.8 which approximates the thermocline depth. (For interpretation of the references to color in this figure legend, the reader is referred to the web version of this article.)

while also responding more strongly to the thermocline position than *G. tumida* (Ravelo and Fairbanks, 1992; Steph et al., 2009; Rincón-Martínez et al., 2011). The optimal calcification temperature seems to be between 16 °C and 19 °C, setting it near the BOPZ in most of the tropics (Patrick and Thunell, 1997; Ravelo and Andreasen, 1999). We find a mean ACD that is near the BOPZ (114 m) with variability reflecting the position of the thermocline at individual core locations (Fig. 3g-h). In Fig. 5b, there is a clear trend in local ACD with thermocline depth, suggesting that *N. dutertrei* calcifies deeper in regions with a deeper thermocline. This is similar to previous findings from multiple studies (Ravelo and Andreasen, 1999; Ravelo and Fairbanks, 1992; Rippert et al., 2016). This species is an opportunistic species that dwells near the chlorophyll maximum, and this depth has been shown to change seasonally along with the nutricline/thermocline, giving an ecological reason for this behavior (Cullen, 2015; Kroon and Ganssen, 1989; Schiebel and Hemleben, 2017). The best fit line fits the data very well, but at a different slope than would be expected if it strictly followed the TP. This suggests that *N. dutertrei* calcification responds to both environmental variables that are linked to the thermocline and those that are more tied directly to depth.

5. Conclusions

Accurate assessments of ACD are necessary to use foraminiferal proxies in a quantitative way to investigate ocean structure. By

compiling data from across the tropics, we investigated the ACD of five species: *G. ruber albus*, *T. sacculifer*, *G. tumida*, *N. dutertrei*, and *P. obliquiloculata*. Despite the large variability introduced by taking data from hydrographically different regions, the mean ACD estimates for each species broadly matched previous regional estimates. The mean and 95% confidence intervals for our ACD estimate for these species are 17 [0, 86] m for *G. ruber*, 48 [0, 128] m for *T. sacculifer*, 210 [123, 385] m for *G. tumida*, 114 [42, 173] m for *N. dutertrei*, and 94 [0, 169] m for *P. obliquiloculata*.

By computing local ACD for each data point, we can start to investigate more complex models of calcification and the biological drivers of calcification. For *G. tumida*, we find that the temperature and position of the thermocline are not important drivers of calcification depth. The calcification depth seems to respond to a variable that is independent of depth, with more variability in the ACD for this species than any other species. *N. dutertrei* and *P. obliquiloculata* respond to thermocline changes, with deeper calcification occurring in locations with a deeper thermocline. Our results confirm existing hypotheses about calcification for these species on a global scale.

These results suggest the possibility of developing predictive models for calcification depth for deep calcifying foraminifera in response to relatively simple environmental variables such as thermocline depth. This may ultimately allow for the direct use of geochemical data from these foraminifera to quantitatively reconstruct vertical profiles of properties in the upper ocean. Improved models for calcification depth

will also allow for more direct comparison between paleoclimate model output and proxy data.

Declaration of Competing Interest

The authors declare that they have no known competing financial interests or personal relationships that could have appeared to influence the work reported in this paper.

Acknowledgements

This work was supported by the National Science Foundation (OCE-1502927, OCE-2002297). Compiled data is available as Supplementary Material as an Excel file and will be archived upon publication at the NOAA/NCEI/World Data Service for Paleoclimatology (<https://www.ncdc.noaa.gov/data-access/paleoclimatology-data>). Analysis code is available on Github (<https://github.com/lakhani1118/Foraminifera-Calcification>).

Appendix A. Supplementary data

Supplementary data to this article can be found online at <https://doi.org/10.1016/j.marmicro.2021.102074>.

References

- Anderson, David M., Mulitza, Stefan, 2001. Compilation of delta 18O data from planktonic foraminifera in surface sediment. PANGAEA. <https://doi.org/10.1594/PANGAEA.60896>.
- Bemis, B.E., Spero, H.J., Bijma, J., Lea, D.W., 1998. Reevaluation of the oxygen isotopic composition of planktonic foraminifera: experimental results and revised paleotemperature equations. *Paleoceanography* 13 (2), 150–160. <https://doi.org/10.1029/98PA00070>.
- Benway, H.M., Mix, A.C., Haley, B.A., Klinkhammer, G.P., 2006. Eastern Pacific Warm Pool paleosalinity and climate variability: 0–30 kyr. *Paleoceanography* 21 (3), 31–55. <https://doi.org/10.1029/2005PA001208>.
- Bijma, J., Faber, W.W., Hemleben, C., 1990. Temperature and salinity limits for growth and survival of some planktonic foraminifers in laboratory cultures. *J. Foraminif. Res.* 20 (2), 95–116. <https://doi.org/10.2113/gsjfr.20.2.95>.
- Boyle, E.A., 1984. Sampling statistic limitations on benthic foraminifera chemical and isotopic data. *Mar. Geol.* 58 (1–2), 213–224. [https://doi.org/10.1016/0025-3227\(84\)90124-5](https://doi.org/10.1016/0025-3227(84)90124-5).
- Broecker, W.S., Clark, E., Lynch-Stieglitz, J., Beck, W., Stott, L.D., Hajdas, I., Bonani, G., 2000. Late glacial diatom accumulation at 9°S in the Indian Ocean. *Paleoceanography* 15 (3), 348–352. <https://doi.org/10.1029/1999PA000439>.
- Brummer, G.J.A., Hemleben, C., Spindler, M., 1987. Ontogeny of extant spinose planktonic foraminifera (Globigerinidae): a concept exemplified by Globigerinoides sacculifer (Brady) and G. ruber (d'Orbigny). *Mar. Micropaleontol.* 12 (C), 357–381. [https://doi.org/10.1016/0377-8398\(87\)90028-4](https://doi.org/10.1016/0377-8398(87)90028-4).
- Cléroux, C., Demenocal, P., Arbuszewski, J., Linsley, B., 2013. Reconstructing the upper water column thermal structure in the Atlantic Ocean. *Paleoceanography* 28 (3), 503–516. <https://doi.org/10.1002/palo.20050>.
- Cornec, M., Claustra, H., Mignot, A., Guidi, L., Lacour, L., Poteau, A., D'Ortenzio, F., Gentili, B., Schmechtig, C., 2021. Deep chlorophyll maxima in the global ocean: occurrences, drivers and characteristics. *Glob. Biogeochem. Cycles* 35 (4), 1–30. <https://doi.org/10.1029/2020GB006759>.
- Cullen, J.J., 2015. Subsurface chlorophyll maximum layers: enduring enigma or mystery solved? *Annu. Rev. Mar. Sci.* 7, 207–239. <https://doi.org/10.1146/annurev-marine-010213-135111>.
- Curry, W.B., Thunell, R.C., Honjo, S., 1983. Seasonal changes in the isotopic composition of planktonic foraminifera collected in Panama Basin sediment traps. *Earth Planet. Sci. Lett.* 64 (1), 33–43. [https://doi.org/10.1016/0012-821X\(83\)90050-X](https://doi.org/10.1016/0012-821X(83)90050-X).
- Dang, H., Jian, Z., Wu, J., Bassinot, F., Wang, T., Kissel, C., 2018. The calcification depth and Mg/Ca thermometry of *Pulleniatina obliquiloculata* in the tropical Indo-Pacific: a core-top study. *Mar. Micropaleontol.* 145 (September), 28–40. <https://doi.org/10.1016/j.marmicro.2018.11.001>.
- Emiliani, C., 1955. Pleistocene temperatures. *J. Geol.* 63 (6), 538–578. <https://doi.org/10.1086/626295>.
- Emiliani, C., Shackleton, N.J., 1974. The Brunhes epoch: isotopic paleotemperatures and geochronology. *Science* 183 (4124), 511–514. <https://doi.org/10.1126/science.183.4124.511>.
- Erez, J., Luz, B., 1983. Experimental paleotemperature equation for planktonic foraminifera. *Geochim. Cosmochim. Acta* 47 (6), 1025–1031. [https://doi.org/10.1016/0016-7037\(83\)90232-6](https://doi.org/10.1016/0016-7037(83)90232-6).
- Farmer, E.C., Kaplan, A., de Menocal, P.B., Lynch-Stieglitz, J., 2007. Corroborating ecological depth preferences of planktonic foraminifera in the tropical Atlantic with the stable oxygen isotope ratios of core top specimens. *Paleoceanography* 22 (3), 1–14. <https://doi.org/10.1029/2006PA001361>.
- Ford, H.L., McChesney, C.L., Hertzberg, J.E., McManus, J.F., 2018. A deep eastern equatorial pacific thermocline during the last glacial maximum. *Geophys. Res. Lett.* 45 (21), 11,806–11,816. <https://doi.org/10.1029/2018GL079710>.
- Gastrich, M.D., 1987. Ultrastructure of a new intracellular symbiotic alga found within planktonic foraminifera. *J. Phycol.* 23 (4), 623–632. <https://doi.org/10.1111/j.1529-8817.1987.tb04215.x>.
- Gibson, K.A., Thunell, R.C., Machain-Castillo, M.L., Fehrenbacher, J., Spero, H.J., Wejnert, K., Nava-Fernández, X., Tappa, E.J., 2016. Evaluating controls on planktonic foraminiferal geochemistry in the Eastern Tropical North Pacific. *Earth Planet. Sci. Lett.* 452, 90–103. <https://doi.org/10.1016/j.epsl.2016.07.039>.
- Hemleben, C., Spindler, M., Anderson, O.R., 1989. Modern Planktonic Foraminifera. Springer-Verlag. <https://doi.org/10.1007/978-1-4612-3544-6>.
- Hollstein, M., Mohtadi, M., Rosenthal, Y., Moffa Sanchez, P., Oppo, D., Martínez Méndez, G., Steinke, S., Hebbeln, D., 2017. Stable oxygen isotopes and Mg/Ca in planktonic foraminifera from modern surface sediments of the Western Pacific Warm Pool: implications for thermocline reconstructions. *Paleoceanography* 32 (11), 1174–1194. <https://doi.org/10.1002/2017PA003122>.
- Jonkers, L., Kučera, M., 2015. Global analysis of seasonality in the shell flux of extant planktonic Foraminifera. *Biogeosciences* 12 (7), 2207–2226. <https://doi.org/10.5194/bg-12-2207-2015>.
- Kawahata, H., Nishimura, A., Gagan, M.K., 2002. Seasonal change in foraminiferal production in the western equatorial Pacific warm pool: evidence from sediment trap experiments. *Deep-Sea Res. II Top. Stud. Oceanogr.* 49 (13–14), 2783–2800. [https://doi.org/10.1016/S0967-0645\(02\)00058-9](https://doi.org/10.1016/S0967-0645(02)00058-9).
- Kessler, S., 1990. Observations of Long Rossby Waves in the Northern Tropical Pacific variability of this, their interpretation propagation processes of Ekman element Evidence waves sets, Section role of long extraequatorial vortices in the north Pacific in terms of simila. *J. Geophys. Res.* 95 (C4), 5183–5217.
- Kim, S.T., O'Neil, J.R., 1997. Equilibrium and nonequilibrium oxygen isotope effects in synthetic carbonates. *Geochim. Cosmochim. Acta* 61 (16), 3461–3475. [https://doi.org/10.1016/S0016-7037\(97\)00169-5](https://doi.org/10.1016/S0016-7037(97)00169-5).
- Kroon, D., Ganssen, G., 1989. Northern Indian Ocean upwelling cells and the stable isotope composition of living planktonic foraminifers. *Deep Sea Res. A, Oceanogr. Res. Papers* 36 (8), 1219–1236. [https://doi.org/10.1016/0198-0149\(89\)90102-7](https://doi.org/10.1016/0198-0149(89)90102-7).
- Kucera, M., Rosell-Melé, A., Schneider, R., Waelbroeck, C., Weinelt, M., 2005. Multiproxy approach for the reconstruction of the glacial ocean surface (MARGO). *Quat. Sci. Rev.* 24 (7–9 SPEC. ISS.), 813–819. <https://doi.org/10.1016/j.quascirev.2004.07.017>.
- Leech, Peter Joseph, 2013. Paleo-Proxies for the Thermocline and Lysocline Over the Last Glacial Cycle in the Western Tropical Pacific Paleo-Proxies for the Thermocline and Lysocline Over the Last Glacial Cycle in the Western.
- Leech, Peter J., Lynch-Stieglitz, J., Zhang, R., 2013. Western Pacific thermocline structure and the Pacific marine Intertropical Convergence Zone during the last Glacial Maximum. *Earth Planet. Sci. Lett.* 363, 133–143. <https://doi.org/10.1016/j.epsl.2012.12.026>.
- LeGrande, A.N., Schmidt, G.A., 2006. Global gridded data set of the oxygen isotopic composition in seawater. *Geophys. Res. Lett.* 33 (12), 1–5. <https://doi.org/10.1029/2006GL026011>.
- Lohmann, G.P., 1995. A model for variation in the chemistry of planktonic foraminifera due to secondary calcification and selective dissolution. *Paleoceanography* 10 (3), 445–457. <https://doi.org/10.1029/95PA00059>.
- Lynch-Stieglitz, J., Curry, W.B., Slowey, N., 1999. A geostrophic transport estimate for the Florida current from the oxygen isotope composition of benthic foraminifera. *Paleoceanography* 14 (3), 360–373.
- Lynch-Stieglitz, J., Polissar, P.J., Jacobel, A.W., Hovan, S.A., Pockalny, R.A., Lyle, M., Murray, R.W., Christina Ravelo, A., Bova, S.C., Dunlea, A.G., Ford, H.L., Hertzberg, J.E., Wertman, C.A., Maloney, A.E., Shackford, J.K., Wejnert, K., Xie, R. C., 2015. Glacial-interglacial changes in central tropical Pacific surface seawater property gradients. *Paleoceanography* 30 (5), 423–438. <https://doi.org/10.1002/2014PA002746>.
- Malevich, S.B., Vetter, L., Tierney, J.E., 2019. Global core top calibration of δ18O in planktonic foraminifera to sea surface temperature. *Paleoceanogr. Paleoclimatol.* 34 (8), 1292–1315. <https://doi.org/10.1029/2019PA003576>.
- Meyers, G., 1979. Annual variation in the slope of the 14°C Isotherm along the Equator in the Pacific Ocean. *J. Phys. Oceanogr.* 9 (5), 885–891. [https://doi.org/10.1175/1520-0485\(1979\)009<0885:AVITSO>2.0.CO;2](https://doi.org/10.1175/1520-0485(1979)009<0885:AVITSO>2.0.CO;2).
- Mohtadi, M., Steinke, S., Groeneveld, J., Fink, H.G., Rixen, T., Hebbeln, D., Donner, B., Herunadi, B., 2009. Low-latitude control on seasonal and interannual changes in planktonic foraminiferal flux and shell geochemistry off south Java: a sediment trap study. *Paleoceanography* 24 (1). <https://doi.org/10.1029/2008PA001636>.
- Mohtadi, M., Oppo, D.W., Lckge, A., Depol-Holz, R., Steinke, S., Groeneveld, J., Hemme, N., Hebbeln, D., 2011. Reconstructing the thermal structure of the upper ocean: Insights from planktic foraminifera shell chemistry and alkenones in modern sediments of the tropical eastern Indian Ocean. *Paleoceanography* 26 (3). <https://doi.org/10.1029/2011PA002132>.
- Monteagudo, M.M., Lynch-Stieglitz, J., Marchitto, T.M., Schmidt, M.W., 2021. Central equatorial pacific cooling during the last glacial maximum. *Geophys. Res. Lett.* 48 (3), 1–10. <https://doi.org/10.1029/2020GL088592>.
- Mulitza, S., Dürkoop, A., Hale, W., Wefer, G., Niebler, H.S., 1997. Planktonic foraminifera as recorders of past surface-water stratification. *Geology* 25 (4), 335–338. [https://doi.org/10.1130/0091-7613\(1997\)025<0335:PFAROP>2.3.CO;2](https://doi.org/10.1130/0091-7613(1997)025<0335:PFAROP>2.3.CO;2).
- Mulitza, S., Boltovskoy, D., Donner, B., Meggers, H., Paul, A., Wefer, G., 2003. Temperature: δ18O relationships of planktonic foraminifera collected from surface waters. *Palaeogeogr. Palaeoclimatol. Palaeoecol.* 202 (1–2), 143–152. [https://doi.org/10.1016/S0031-0182\(03\)00633-3](https://doi.org/10.1016/S0031-0182(03)00633-3).

- Patrick, A., Thunell, R.C., 1997. Tropical Pacific sea surface temperature and upper water column thermal structure during the last glacial maximum. *Paleoceanogr. Paleoclimatol.* 12 (5), 649–657. <https://doi.org/10.1029/97PA01553>.
- Ravelo, A.C., Andreasen, D.H., 1999. Using planktonic foraminifera as monitors of the tropical surface ocean. *Reconstruct. Ocean History* 217–243. https://doi.org/10.1007/978-1-4615-4197-4_14.
- Ravelo, A.C., Fairbanks, R.G., 1992. Oxygen isotopic composition of multiple species of planktonic foraminifera: recorders of the modern photic zone temperature gradient. *Paleoceanography* 7 (6), 815–831. <https://doi.org/10.1029/92PA02092>.
- Ravelo, A.C., Fairbanks, R.G., Philander, S.G.H., 1990. Reconstructing tropical Atlantic hydrography using planktonic foraminifera and an ocean model. *Paleoceanography* 5 (3), 409–431. <https://doi.org/10.1029/PA005I003p00409>.
- Regenberg, M., Steph, S., Nürnberg, D., Tiedemann, R., Garbe-Schönberg, D., 2009. Calibrating Mg/Ca ratios of multiple planktonic foraminiferal species with $\delta^{18}\text{O}$ -calcification temperatures: paleothermometry for the upper water column. *Earth Planet. Sci. Lett.* 278 (3–4), 324–336. <https://doi.org/10.1016/j.epsl.2008.12.019>.
- Rincón-Martínez, D., Steph, S., Lamy, F., Mix, A., Tiedemann, R., 2011. Tracking the equatorial front in the eastern equatorial Pacific Ocean by the isotopic and faunal composition of planktonic foraminifera. *Mar. Micropaleontol.* 79 (1–2), 24–40. <https://doi.org/10.1016/j.marmicro.2011.01.001>.
- Rippert, N., Nürnberg, D., Raddatz, J., Maier, E., Hathorne, E., Bijma, J., Tiedemann, R., 2016. Constraining foraminiferal calcification depths in the western Pacific warm pool. *Mar. Micropaleontol.* 128, 14–27. <https://doi.org/10.1016/j.marmicro.2016.08.004>.
- Russell, A.D., Emerson, S., Nelson, B.K., Erez, J., Lea, D.W., 1994. Uranium in foraminiferal calcite as a recorder of seawater uranium concentrations. *Geochim. Cosmochim. Acta* 58 (2), 671–681. [https://doi.org/10.1016/0016-7037\(94\)90497-9](https://doi.org/10.1016/0016-7037(94)90497-9).
- Sagawa, T., Yokoyama, Y., Ikebara, M., Kuwae, M., 2012. Shoaling of the western equatorial Pacific thermocline during the last glacial maximum inferred from multispecies temperature reconstruction of planktonic foraminifera. *Palaeogeogr. Palaeoclimatol. Palaeoecol.* 346–347, 120–129. <https://doi.org/10.1016/j.palaeo.2012.06.002>.
- Savin, S.M., Douglas, R.G., 1973. Stable isotope and magnesium geochemistry of recent Planktonic Foraminifera from the South Pacific. *Bull. Geol. Soc. Am.* 84 (7), 2327–2342. [https://doi.org/10.1130/0016-7606\(1973\)84<2327:SIAMGO>2.0.CO;2](https://doi.org/10.1130/0016-7606(1973)84<2327:SIAMGO>2.0.CO;2).
- Schiebel, R., Hemleben, C., 2005. Modern planktic foraminifera. *Paläontol. Z.* 79 (1), 135–148. <https://doi.org/10.1007/bf03021758>.
- Schiebel, R., Hemleben, C., 2017. Planktic foraminifers in the modern ocean. In: *Planktic Foraminifers in the Modern Ocean*. <https://doi.org/10.1007/978-3-662-50297-6>.
- Schmidt, G.A., Mulitza, S., 2002. Global calibration of ecological models for planktic foraminifera from coretop carbonate oxygen-18. *Mar. Micropaleontol.* 44 (3–4), 125–140. [https://doi.org/10.1016/S0377-8398\(01\)00041-X](https://doi.org/10.1016/S0377-8398(01)00041-X).
- Sil, S., Chakraborty, A., 2012. The mechanism of the 20°C isotherm depth oscillations for the Bay of Bengal. *Mar. Geod.* 35 (3), 233–245. <https://doi.org/10.1080/01490419.2011.637865>.
- Spero, H.J., Mielke, K.M., Kalve, E.M., Lea, D.W., Pak, D.K., 2003. Multispecies approach to reconstructing eastern equatorial Pacific thermocline hydrography during the past 360 kyr. *Paleoceanography* 18 (1). <https://doi.org/10.1029/2002PA000814>.
- Stainbank, S., Kroon, D., Rüggeberg, A., Raddatz, J., De Leau, E.S., Zhang, M., Spezzaferri, S., 2019. Controls on planktonic foraminifera apparent calcification depths for the northern equatorial Indian Ocean. In: *PLoS One* 14 (9). <https://doi.org/10.1371/journal.pone.0222299>.
- Steinhardt, J., de Nooijer, L.L.J., Brummer, G.-J., Reichart, G.-J., 2015. Profiling planktonic foraminiferal crust formation. *Geochem. Geophys. Geosyst.* 16 (7), 2409–2430. <https://doi.org/10.1002/2015GC005752>.
- Steph, S., Regenberg, M., Tiedemann, R., Mulitza, S., Nürnberg, D., 2009. Stable isotopes of planktonic foraminifera from tropical Atlantic/Caribbean core-tops: Implications for reconstructing upper ocean stratification. *Mar. Micropaleontol.* 71 (1–2), 1–19. <https://doi.org/10.1016/j.marmicro.2008.12.004>.
- Waelbroeck, C., Mulitza, S., Spero, H., Dokken, T., Kieffer, T., Cortijo, E., 2005. A global compilation of late Holocene planktonic foraminiferal $\delta^{18}\text{O}$: Relationship between surface water temperature and $\delta^{18}\text{O}$. *Quat. Sci. Rev.* 24 (7–9 SPEC. ISS), 853–868. <https://doi.org/10.1016/j.quascirev.2003.10.014>.
- Watkins, J.M., Mix, A.C., Wilson, J., 1998. Living planktic foraminifera in the central tropical Pacific Ocean: Articulating the equatorial “cold tongue” during La Niña, 1992. *Mar. Micropaleontol.* 33 (3–4), 157–174. [https://doi.org/10.1016/S0377-8398\(97\)00036-4](https://doi.org/10.1016/S0377-8398(97)00036-4).
- Weijnert, K.E., Thunell, R.C., Astor, Y., 2013. Comparison of species-specific oxygen isotope paleotemperature equations: sensitivity analysis using planktonic foraminifera from the Cariaco Basin, Venezuela. *Mar. Micropaleontol.* 101, 76–88. <https://doi.org/10.1016/j.marmicro.2013.03.001>.
- Zhang, P., Zuraida, R., Xu, J., Yang, C., 2016. Stable carbon and oxygen isotopes of four planktonic foraminiferal species from core-top sediments of the Indonesian throughflow region and their significance. *Acta Oceanol. Sin.* 35 (10), 63–75. <https://doi.org/10.1007/s13131-016-0890-1>.
- Zhang, L., Delworth, T.L., Cooke, W., Yang, X., 2019a. Natural variability of Southern Ocean convection as a driver of observed climate trends. *Nat. Clim. Chang.* 9 (1), 59–65. <https://doi.org/10.1038/s41558-018-0350-3>.
- Zhang, P., Zuraida, R., Rosenthal, Y., Holbourn, A., Kuhnt, W., Xu, J., 2019b. Geochemical characteristics from tests of four modern planktonic foraminiferal species in the Indonesian Throughflow region and their implications. *Geosci. Front.* 10 (2), 505–516. <https://doi.org/10.1016/j.gsf.2018.01.011>.